

A Data-driven Approach to Risk-aware Robust Design

Luis G. Crespo, Bret Stanford, Natalia Alexandrov

NASA Langley Research Center, Hampton, VA, 23681

This paper proposes risk-averse and risk-agnostic formulations to robust design in which solutions that satisfy the system requirements for a set of scenarios are pursued. These scenarios, which correspond to realizations of uncertain parameters or varying operating conditions, can be obtained either experimentally or synthetically. The proposed designs are made robust to variations in the training data by considering perturbed scenarios. This practice allows accounting for error and uncertainty in the measurements, thereby preventing data overfitting. Furthermore, we use relaxation to trade-off a lower optimal objective value against lesser robustness to uncertainty. This is attained by eliminating a given number of optimally chosen outliers from the dataset, and by allowing for the perturbed scenarios to violate the requirements with an acceptably small probability. For instance, we can pursue a riskier design that attains a lower objective value in exchange for a few scenarios violating the requirements, or we might seek a more conservative design that satisfies the requirements for as many perturbed scenarios as possible. The design of a flexible wing subject to aeroelastic constraints is used for illustration.

I. Introduction

Let $J : \Theta \rightarrow \mathbb{R}$ be an objective function of the decision variable $\theta \in \mathbb{R}^{n_\theta}$. Furthermore, let $r_k(\theta, \delta) : \mathbb{R}^{n_\theta} \times \mathbb{R}^{n_\delta} \rightarrow \mathbb{R}$ for $k = 1, \dots, n_r$ be a continuous function associated with a system requirement, where the parameter $\delta \in \mathbb{R}^{n_\delta}$ is subject to aleatory uncertainty. The optimization program under consideration is

$$\begin{aligned} \min_{\theta \in \Theta} \quad & J(\theta) \\ \text{subject to:} \quad & r_k(\theta, \delta) \leq 0, \quad k = 1, \dots, n_r, \end{aligned} \tag{1}$$

for most of the elements of δ in $\Delta \subset \mathbb{R}^{n_\delta}$. The particular subset of Δ containing such elements will be specified below. The objective and constraints of (1) are assumed to be continuous functions of θ , thereby making standard gradient based algorithms applicable to the forthcoming formulations.

Denote as θ^* the solution to (1). The *feasible set* of (1) corresponding to a parameter point δ is

$$\mathcal{X}(\delta) = \{\theta \in \Theta : r_k(\theta, \delta) \leq 0, \quad k = 1, \dots, n_r\}. \tag{2}$$

Hence, $\mathcal{X}(\delta)$ is comprised of all the decision (or design) points that satisfy the constraints for the parameter point δ . The *success domain* of (1) corresponding to the decision point θ is

$$\mathcal{S}(\theta) = \bigcap_{k=1}^{n_r} \mathcal{S}_k(\theta), \quad (3)$$

where $\mathcal{S}_k(\theta) = \{\delta \in \Delta : r_k(\theta, \delta) \leq 0\}$. Hence, $\mathcal{S}(\theta)$ is comprised of all the parameter points for which the decision point θ satisfies the constraints. The set Δ is partitioned into the success domain and the *failure domain*, \mathcal{F} , so $\mathcal{F}(\theta) \cup \mathcal{S}(\theta) = \Delta$ and $\mathcal{F}(\theta) \cap \mathcal{S}(\theta) = \emptyset$. Each of the sets in the right-hand side of (3) is an individual success domain, with their complement being the corresponding individual failure domain.

The field of optimization under uncertainty, which entails solving (1) for a given Δ , was pioneered in the 1950s by Dantzig [1] and Charnes [2], who set the foundations for *Robust Optimization* (RO) and *Chance Constrained Optimization* (CCO), respectively.

RO [3, 4, 5] seeks a design that satisfies the constraints for all $\delta \in \Delta$. The main advantage of such designs is the guarantee that the requirements are satisfied for all possible uncertainty realizations. However, RO programs are generally intractable even when the requirement functions are convex, e.g., the robust counterpart of a second order cone program with polyhedral uncertainty is NP hard [6, 7, 8] (tractable linear RO problems, which require a suitably chosen Δ and particular forms for $r_k(\theta, \delta)$, are summarized in [9, 10]). In addition to such challenges, the resulting design commonly underperforms other designs for most elements of δ in Δ .

In contrast, CCO seeks a design that allows for some elements of Δ to violate the requirements [11, 12]. In particular, it replaces the constraints in (1) with $\mathbb{P}_\delta[\mathcal{S}(\theta)] \geq 1 - \epsilon$, where \mathbb{P}_δ is the distribution of δ , and $0 < \epsilon \ll 1$. This constraint in turn, implies that the system requirements are satisfied by most uncertainty realizations of δ on Δ . Distributions also enable the analyst to consider objective functions and constraints depending on moments of a response function [13, 14, 15]. CC designs reduced the intrinsic conservatism of RO designs by ignoring some of the worst-case realizations of the uncertainty, thereby lowering the objective function. The main difficulty in solving CCO programs stems from the inability to evaluate such constraints with high accuracy. This task entails calculating a high dimensional integral over a complex integration domain, a problem that is known to be strongly NP-hard [16, 17]. Furthermore, the feasible set of a CCO program is often non-convex, making the identification of the global optimum difficult. In fact, the feasible set of a chance constraint corresponding to a convex constraint, i.e., $r(\theta, \delta) \leq 0$ is convex in θ for any δ , might be non-convex^a. CCO programs taking special forms that make the feasible set convex can be efficiently solved [19, 20, 21, 22, 23, 24]. However, many engineering problems of interest do not take such forms. In spite of the above drawbacks, the ability to relax the robustness specifications enforced by RO, thereby to reduce the potentially high conservatism of a design synthesized for the worst-case combination of uncertainties, makes CCO an important and practical tool for decision making under uncertainty [25, 26].

A particular case of CCO, called *Reliability-Based Design Optimization* (RBDO), seeks designs that minimize the probability of failure. These applications often consider implicit

^aThe convexity of the requirement functions is preserved by reformulating the CC in terms of the *Conditional Value at Risk* (CVaR) at the expense of reducing the feasible set [11, 18]. In contrast to CCs, however, CVaR-based constraints make the resulting design risk-averse, e.g., θ^* depends on a risk measure taking values on the set $\{\delta : r(\theta^*, \delta) > 0\}$.

non-convex requirement functions whose evaluation requires a numerical simulation. RBDO methods [27] seek designs having an acceptably low failure probability for a distribution \mathbb{P}_δ set upfront. A standard approach to RBDO involves two nested loops: an outer loop that searches for an optimal design, and an inner loop that evaluates $\mathbb{P}_\delta[\mathcal{F}(\theta)]$ for every candidate design chosen by the outer loop [28]. This evaluation is often called a reliability analysis. The high computational cost of accurately estimating small probabilities makes RBDO expensive. Decoupling approaches [29], single-loop methods [30, 31, 32], and efficient approximations to the failure probability have been used to make RBDO more efficient. Single-loop methods combine the outer and inner loops by substituting the reliability analysis with an approximation [33], whereas decoupling methods replace the nested optimization with a sequence of deterministic programs [34]. Some of the approaches used to reduce the computational cost of the inner loop include subset simulation [35], line sampling [36], importance sampling [37], first-order and second-order reliability methods [28, 38, 39, 40], multi-fidelity surrogate-modeling strategies [41, 42, 43, 44], and many others [45, 46, 47].

An important drawback of the RO and CCO approaches is the high sensitivity of the resulting design to the assumed uncertainty model, i.e. Δ and \mathbb{P}_δ respectively. In the CCO case, the prescription of a distribution generally involves learning a random vector, a dependency structure, and tail model from data. This process is challenging when n_δ is large, when parameter dependencies are strong, when the dataset is incomplete (the dependency between disjoint subsets of data cannot be measured) or when the data are scarce. Poorly chosen uncertainty models might lead to designs that grossly underperform in practice [48, 49]. Non-probabilistic models and mixtures of non-probabilistic and probabilistic models have been used when the data are scarce [50, 51, 52, 53]. These models make use of evidence theory [54, 55], possibility theory [56], credal sets, fuzzy sets and ambiguity sets theory [57, 58, 59]. The subjectivity in prescribing such a distribution can be mitigated by using distributionally robust approaches, which seek to identify designs that satisfy the requirements for a family of distributions [60, 61, 62].

II. Solution Strategy and Goals

The strategies proposed below are data-driven. Data-driven methods include the scenario approach [20, 63, 64, 65, 66], the sample average approximation [67], and robust optimization over safe approximations of the feasible CC set [68]. Developments in the latter two categories, however, have mostly focused on convex requirement functions taking particular forms. The strategies proposed below, which belong to the former category, do not suffer from such restrictions, thereby being broadly applicable.

Scenario-based strategies make direct use of a finite number of realizations of δ . This practice eliminates the subjectivity introduced by having to model the uncertainty in δ as either a set or a distribution^b from data. More importantly, these strategies offer a computationally cheaper alternative to RBDO approaches while yielding a feasibility guarantee [66]. These realizations, called the *nominal* scenarios, comprise the dataset

$$\mathcal{D} = \{\delta^{(i)}\}_{i=1}^n. \quad (4)$$

^bWhen such realizations are unavailable, samples drawn from a synthetic distribution could be used instead.

The nominal scenarios are assumed to be *Independent and Identically Distributed* (IID) observations drawn from an unknown distribution \mathbb{P}_δ . Hence, we will solve (1) for $\Delta = \mathcal{D}$ hoping that the resulting design θ^* will satisfy the requirements for neighboring scenarios beyond those used for training.

The main goals of this article are two-fold. First, we want to safeguard the robust design against data overfitting. This is of particular interest when the metrology system is inaccurate, e.g., systems commonly used in biological and environmental applications [69, 70, 71, 72, 73, 74], and when the measurements are noisy [75]. Another situation when overfitting must be prevented arises when the computational cost of evaluating the objective function and/or the requirements is high, thereby limiting the analyst to use a small number of scenarios. Insufficient and inaccurately measured data threaten the relevance of a data-driven design because such a design might be infeasible in practice or it might attain an objective value far greater than the one predicted. These anomalies will be mitigated by considering *perturbed* scenarios. In particular, we wish to prevent θ^* from overfitting \mathcal{D} by ensuring that the success domain $\mathcal{S}(\theta^*)$ not only contains the scenarios therein but also the vicinity around them.

Second, we want to explore the trade-off between performance and robustness by solving (1) for only a fraction of the n scenarios. By making this fraction as large as possible we obtain the most robust design and a comparatively large $J(\theta^*)$. However, this value can be lowered by considering a smaller fraction. The scenarios excluded from this fraction, called outliers^c, will be chosen optimally during the search for θ^* by using risk-averse or risk-agnostic formulations. These formulations account for or ignore the loss resulting from the elimination of outliers respectively. The elimination of outliers mitigates the detrimental effects that extreme observations often have on data-driven designs [76, 77, 78]. And when data is unavailable and we must assume a distribution \mathbb{P}_δ to obtain synthetic scenarios, the elimination of outliers reduces the potentially high sensitivity of θ^* to this assumption.

This paper is organized as follows. Section III introduces a few uncertainty model types for the perturbed scenarios. This is followed by Section IV, where the strategies proposed are qualitatively explained using an engineering example. Several risk-averse and risk-agnostic formulations to robust design are presented and exemplified in Sections V and VI. The reliability analysis of the resulting designs is studied in Section VII. This analysis enables the designer to determine if the resulting design meets the reliability specifications imposed upon the system. If this is not the case, he/she can either expand the training set \mathcal{D} or choose a better design architecture before redesigning. Finally, we state a few conclusions and outline some directions of future work.

III. Modeling Uncertainty in the Data

The pursuit of a design that remains feasible when the data are perturbed, a property called *robustness* hereafter, entails modeling such perturbations. An uncertainty model should be prescribed according to the accuracy and precision of the metrology system, and/or to the analyst's belief of where the true value of δ might be. While overly small perturbations

^cNote that this definition is rooted on the feasibility of a scenario instead of its relationship to other scenarios (an outlier is commonly defined as a point that does not follow the trends followed by most of the data).

might lead to designs that violate the requirements in practice, overly large perturbations might lead to conservative designs having an unnecessarily high $J(\theta^*)$.

One model class is given by compact sets. Denote $\delta_s^{(i)} = \{\delta : \|\delta - \delta^{(i)}\| \leq \ell^{(i)}\}$ as the model of a perturbed scenario, where $\ell^{(i)} \geq 0$ is given by a rule that might depend on $\delta^{(i)}$. For instance, $\delta_s^{(i)}$ might be a ball centered at $\delta^{(i)}$ of fixed radius. As such, $\delta_s^{(i)}$ is fully prescribed by a realization of the unknown distribution \mathbb{P}_δ . This model class leads to the sequence

$$\mathcal{D}_s = \left\{ \delta_s^{(i)} \right\}_{i=1}^n. \quad (5)$$

Another model class is given by distributions. Denote $\delta_d^{(i)}$ as a random vector having $\delta_s^{(i)}$ as the support set. Hence, the uncertainty model $\delta_d^{(i)}$ is prescribed by a realization of the unknown distribution \mathbb{P}_δ and a distribution $\mathbb{P}_{\delta^{(i)}}$ set by the analyst. For instance, $\delta_d^{(i)}$ might be a Normal distribution having $\delta^{(i)}$ as its mean and a fixed covariance matrix. This model class leads to the sequence

$$\mathcal{D}_d = \left\{ \delta_d^{(i)} \right\}_{i=1}^n. \quad (6)$$

Designs that are robust to uncertainty in δ can be pursued by various means. The strategies below make use of a multi-point representation of (6). Let $\delta_p^{(i)} = \{\delta^{(i,j)}\}_{j=1}^m$ be a collection of m sample points drawn from $\delta_d^{(i)}$. This leads to the multi-point sequence

$$\mathcal{D}_p(m) = \left\{ \delta_p^{(i)} \right\}_{i=1}^n. \quad (7)$$

An element of (5), (6) or (7) will be called a *perturbed* scenario.

This representation of the uncertainty may introduce an error in the resulting design, e.g., $\delta_p^{(i)} \subset \mathcal{S}(\theta^*)$ but $\delta_s^{(i)} \not\subset \mathcal{S}(\theta^*)$. This outcome might be eliminated by increasing n or by using sample points outside the support set. Unfortunately, the semi-infinite programming approaches that eliminate this error are inapplicable to general requirement functions.

The forthcoming programs are reformulations of

$$\begin{aligned} \min_{\theta \in \Theta} \quad & J(\theta) \\ \text{subject to:} \quad & r_k(\theta, \delta^{(i,j)}) \leq 0, \text{ for most } \delta^{(i,j)} \in \mathcal{D}_p, k = 1, \dots, n_r, \end{aligned} \quad (8)$$

in which a particular subset of the scenarios in \mathcal{D}_p are chosen as outliers. This selection, which is made optimally as θ^* is searched for, might depend on the severity of the corresponding requirement violation. This feature is explained next. Risk is commonly defined as the probability of an adverse outcome times the corresponding “loss” or consequence. In the context of this paper, the adverse outcome is the violation of a requirement, whereas the loss measure is the corresponding positive value taken by $r(\theta, \delta)$. A design θ^* that depends on a loss measure will be called *risk-averse*. This dependency limits the extent by which the outliers are allowed to violate the requirements. In contrast, formulations in which θ^* does not depend on a loss measure will be called *risk-agnostic*.

Hereafter, the set of outliers will be denoted as $\mathcal{O} \subset \{1, \dots, n\}$ with $|\mathcal{O}| = n_o$, whereas its complement set, $I = \{1, \dots, n\} \setminus \mathcal{O}$ with $|I| = n_i$, will denote the set of inliers.

The data sequence in (8) lead to the following classification: (i) design points computed from a single scenario will be called *single-point* (ii) design points computed from more than one scenario will be called *multi-point*, and (iii) multi-point designs for which $m > 1$ will be called *multi-point-robust*.

IV. Motivational Example

Consider the design of an aeroelastic wing subject to a structural dynamic constraint. In this setting, the decision variable θ parameterizes the wing’s geometry, whereas the parameter δ is comprised of structural damping coefficients, which are intrinsically uncertain, and the Mach number, which varies with the flying condition. The objective function $J(\theta)$ is the mass of the wing, and $r_1(\theta, \delta) > 0$ implies flutter instability. Therefore, we seek to design a wing of minimal mass that is stable for (most of) the n scenarios in \mathcal{D} .

A multi-point wing design that satisfies the requirement for as many scenarios as possible can be obtained by using the formulations in^d Section V. These formulations not only render θ_1^* but also the corresponding $n_{o,1}$ outliers. The underlying physics or the wing’s parameterization might cause $n_{o,1}$ to be greater than zero. If this outcome is unacceptable, other design architectures should be considered. Assume that $n_{o,1}$ is acceptably low. At this point the analyst might wonder how much lighter the wing could be if we let the wing flutter for a few more scenarios. The same formulations can be used to derive design θ_2^* having $n_{o,2} > n_{o,1}$ outliers. It might turn out that $J(\theta_2^*)$ is considerably smaller than $J(\theta_1^*)$. At this point it is well worth pondering if the mass reduction $J(\theta_1^*) - J(\theta_2^*)$ justifies the loss in robustness caused by increasing the number of outliers from $n_{o,1}$ to $n_{o,2}$.

Imagine now that if the n scenarios in \mathcal{D} are allowed to vary uniformly no more than 5% from their nominal value, the wing design θ_2^* will fail for $n_{o,2'} > n_{o,2}$ of them, i.e., at least one out of the m parameter points from the $n_{o,2'}$ perturbed scenarios falls into the failure domain. The high sensitivity of θ_2^* to variations in the training data \mathcal{D} might render this wing unacceptable. Hence, a multi-point-robust wing is designed by using the formulations in Sections V.A or V.C. Say, the resulting wing θ_3^* violates the requirements for $n_{o,3}$ perturbed scenarios with probability $1 - \gamma$, where $n_{o,3}$ is as small as possible and $0 \ll \gamma < 1$. As before, the physics might prevent $n_{o,3}$ from being zero. Designs having a lower mass and less robustness to uncertainty can be sought by lowering γ and/or increasing $n_{o,3}$.

Either physics-based limitations or choice might make a scenario an outlier. The process by which outliers are selected within the proposed formulations might depend on a risk (or loss) measure (See Section V.A) or not (See Sections V.C or V.D). This measure quantifies the consequence of an adverse outcome, which in the context of this paper is the positive value of $r_1(\delta, \theta)$ attained by an outlier. For instance, a risk-averse approach seeks to lower $\ell = \mathbb{E}[r_1(\delta^{(i,j)}, \theta) | r_1(\delta^{(i,j)}, \theta) > 0]$, where $\mathbb{E}[\cdot]$ is the sample mean. In the context of this example, ℓ measures the strength of the instability. Conversely, a risk-agnostic approach will ignore the possibly large values that this measure might take, e.g., a design that minimizes the empirical probability of instability, $\sum_{i=1}^n I[\max_j r_1(\delta^{(i,j)}, \theta) > 0]/n$, where $I[\cdot]$ is the indicator function. Risk-averse and risk-agnostic approaches might lead to designs having a comparable probability of failure but very different objective values and loss measures.

Furthermore, we might consider a wing design in which δ also contains material properties, thereby making the objective function also depend on δ . The developments in Section VI enable seeking the wing of minimal expected mass after the same outliers are eliminated from both the objective and the requirement functions. The final design should be chosen from several design alternatives having varying degrees of robustness and performance after

^dUse $J = 0$ when the formulation is risk-averse, and $J = \|\alpha\|$ when the formulation is risk-agnostic after making α an additional decision variable. These settings lead to designs that minimize the sum of the individual probabilities of failure.

comparing their objective function value, number of outliers, and loss measures. A realistic wing design example is presented below. In the remainder of this paper, we detail the formulations leading to such designs.

V. Moment-independent Optimization Programs

In this section we present risk-averse and risk-agnostic reformulations of (8). The resulting CCed programs use approximations to the *Cumulative Distribution Function* (CDF) of a random variable z and its inverse based on the function evaluations in $\mathcal{Z} = \{z^{(i)}\}_{i=1}^n$. These approximations, denoted as $F_{\mathcal{Z}}$ and $F_{\mathcal{Z}}^{-1}$ respectively hereafter, are detailed in the Appendix.

V.A. Risk-averse Scenario-based Formulation

Consider the optimization program

$$\begin{aligned} \langle \theta^*, \xi^* \rangle = \operatorname{argmin}_{\theta \in \Theta, \xi \geq 0} \quad & J(\theta) + \rho \sum_{i=1}^n \xi_i \\ \text{subject to:} \quad & F_{\mathcal{Z}_A(\theta, \delta_p^{(i)}, k)}^{-1}(\gamma_k) \leq \xi_i, \quad i = 1, \dots, n, \quad k = 1, \dots, n_r, \end{aligned} \quad (9)$$

where $\rho \in \mathbb{R}$ is a penalty parameter, $\xi \in \mathbb{R}^n$ is a slack variable,

$$\mathcal{Z}_A(\theta, \delta_p^{(i)}, k) \triangleq \left\{ r_k(\theta, \delta^{(i,j)}) \right\}_{j=1}^m, \quad (10)$$

is the sequence of function evaluations of the k th requirement for all sample points of the i th scenario, and $0 \ll \gamma_k \leq 1$ is the minimally acceptable probability of success for such a requirement^e. Hence, (9) seeks a design that minimizes the sum of J and a penalty term while bounding the individual success probabilities for most elements of (7) from below. Note that a constraint of (9) corresponding to a fixed i and a fixed k for $\xi_i = 0$ is a computationally tractable heuristic for $\mathbb{P}_{\delta^{(i)}}[\mathcal{S}_k(\theta)] \geq \gamma_k$. The CC in (9) is a reformulation of the constraints in (1), in which “most” refers to a subset of Δ where the k th requirement function is satisfied by the perturbed scenarios with probability no less than γ_k .

Outliers are the scenarios for which at least one of the individual probabilities of success is below the acceptable threshold:

$$\mathcal{O} = \left\{ i \in \{1, \dots, n\} : \max_{k=1, \dots, n_r} F_{\mathcal{Z}_A(\theta, \delta_p^{(i)}, k)}^{-1}(\gamma_k) > 0 \right\}. \quad (11)$$

This is equivalent to $\mathcal{O} = \{i \in \{1, \dots, n\} : \xi_i^* > 0\}$. When $\gamma_k < 1$ a few points of $\delta_p^{(i)}$ might fall into the failure domain regardless of such a scenario being an outlier or not.

Relaxation entails turning an optimization program into one with either looser constraints or fewer constraints, so the feasible set is enlarged and the objective value $J(\theta^*)$ is potentially lower. The feasible set of (9) is

$$\mathcal{X}_{\text{robust}} = \bigcap_{i \in A, j \in B} \mathcal{X}(\delta^{(i,j)}), \quad (12)$$

^eThe CC in (9) is equivalent to $\mathbb{P}_{\delta}[r_k(\theta, \delta) \leq \xi_i] = F_{\mathcal{Z}_A(\theta, \delta_p^{(i)}, k)}(\xi_i) \geq \gamma_k$. Note that the value taken by the CDF might plateau at zero or one as θ is varied, thereby making gradient-based searches stop at a local extremum. As such, CCs are better cast in terms of the inverse CDF.

where \mathcal{X} was defined in (2). Program (9) carries out two types of relaxation. The first type reduces the elements of A in (12) by lowering ρ . In particular, (9) enables the analyst to obtain various solutions as ρ is varied from zero (no regret for having probabilities of success below γ_k) to infinite (infinite regret for having probabilities of success below γ_k). Large values of ρ will drive the ξ_i 's near zero, thereby ensuring that as many success probabilities for the k th requirement as possible are no less than γ_k . Moderately large values of ρ will make some $\xi_i^* > 0$, therefore yielding a design for which some probabilities are below γ_k . Hence, depending on the value of ρ , some perturbed scenarios are allowed to violate the requirements beyond acceptable limits for the purpose of lowering $J(\theta^*)$. However, this action has itself a cost, as expressed by the auxiliary variables ξ_i : if $\xi_i > 0$ the constraint $F_{\mathcal{Z}_A}^{-1}(\gamma_k) \leq 0$ is relaxed to $F_{\mathcal{Z}_A}^{-1}(\gamma_k) \leq \xi_i$ in exchange for a cost increase of $\rho \xi_i$. Note that the dependency of the number of outliers n_o on ρ is implicit. The second relaxation type reduces the elements of B in (12) by setting the value of γ_k for $k = 1, \dots, n_r$ so requirement violations for a fixed fraction of the m points in $\delta_p^{(i)}$ are allowed.

Therefore, the feasible set of (9) is given by (12) with $A \subseteq \{1, \dots, n\}$, and $B(i) \subset \{1, \dots, m\}$. The expansion of this set for an optimally chosen set of outliers and an optimally chosen fraction of the points in $\delta_p^{(i)}$ for $i = 1, \dots, n$ might yield a considerably lower objective value without impacting most of the data, i.e., the probability of failure corresponding to most perturbed scenarios is not affected by these choices.

Program (9) might not have a solution for which all ξ_i^* are zero, thereby making relaxation crucial. Relaxation enables the analyst to pursue the most robust design of a given architecture, as well as the identification of the scenarios for which the design specifications cannot be met. Notice that the number of decision variables in (9) grows with the number of scenarios, thereby limiting its applicability to moderately large datasets.

The non-zero terms in the summation measure the extent by which the outliers violate the requirements, thereby making (9) risk-averse. In this context, the adverse outcome is the violation of a requirement with an unacceptably large probability, whereas ξ_i is the loss measure. Hence, the dependency of the penalty term on ξ makes θ^* a risk-averse design.

The optimization program (9) has $n \times n_r$ individual CCs. Using the joint CC $\mathbb{P}_\delta[\max_k r_k(\theta, \delta) \leq \xi_i] \geq \gamma$ for $i = 1, \dots, n$, yields a program having a greater feasible set and thus a possibly lower $J(\theta^*)$. This is a consequence of the Bonferroni inequality, $\mathbb{P}_\delta[\mathcal{F}(\theta)] \leq \sum_i \mathbb{P}_\delta[\mathcal{F}_i(\theta)]$. Therefore replacing a joint CC with individual CCs introduces conservatism in the resulting design. This paper uses individual CCs because (i) they are simpler to implement, (ii) formulations based on the inverse CDF, easily computable in one dimension, lower the chance of the converged θ^* being a local minima (See footnote 7), and (iii) the minimally acceptable probability of success γ_k might not be the same for all requirements. Note however, that all the proposed formulations could use a joint CC instead (after using the multi-variate extension of (31)).

V.A.1. Worst-case formulation

The optimization program (9) with $\gamma_k = 1$ for $k = 1, \dots, n_r$ is equivalent to

$$\begin{aligned} \langle \theta^*, \xi^* \rangle = \operatorname{argmin}_{\theta \in \Theta, \xi \geq 0} \quad & J(\theta) + \rho \sum_{i=1}^n \xi_i & (13) \\ \text{subject to:} \quad & r_k(\theta, \delta^{(i,j)}) \leq \xi_i, \quad i = 1, \dots, n, \quad j = 1, \dots, m, \quad k = 1, \dots, n_r. \end{aligned}$$

This formulation [79] is called “worst-case” because ξ_i^* depends on the element of $\delta_p^{(i)}$ at which the requirement function takes on the greatest value. A few remarks on this particular case are discussed next.

Note that the m constraints corresponding to a fixed i and a fixed k for $\xi_i = 0$ are a computationally tractable heuristic for $\delta_s^{(i)} \subset \mathcal{S}_k(\theta)$. As such, (13) is an approximation to the semi-infinite program with constraints $r_k(\theta, \delta) \leq \xi_i$ for all $\delta \in \delta_s^{(i)}$, $i = 1, \dots, n$ and $k = 1, \dots, n_r$. Furthermore, the elements of \mathcal{D}_p having at least one parameter point in the failure domain will be the outliers. In contrast to (9), (13) is a convex program when the requirement functions are convex.

The feasible set of (13) is given by (12) with $A \subseteq \{1, \dots, n\}$ and $B = \{1, \dots, m\}$. Hence, relaxation is only attained by eliminating outliers. As such, it only takes a single element of $\delta_p^{(i)}$ falling into the failure domain for (13) to penalize a requirement violation. The relaxation of B in (12) might make CC designs differ considerably from worst-case designs in (13) for the same number of outliers. The possibly significant lower value $J(\theta^*)$ of a CC design along with some risk tolerance might render it preferable unless safety is paramount [80].

V.B. Risk-Averse Requirement-based Formulation

The number of decision variables in the above formulations grows with the number of scenarios, rendering them impractical when the dataset is large. Furthermore, the loss measure in the penalty term is driven by the greatest values taken by the requirement functions, thereby possibly making a few requirements dominate the others. This problem can be avoided by scaling these functions, a difficult task due to their dependency on θ . The formulation below eliminates these drawbacks.

Consider the CC program

$$\begin{aligned} \langle \theta^*, \zeta^* \rangle = \operatorname{argmin}_{\theta \in \Theta, 0 \leq \zeta \leq 1} & J(\theta) + \rho^\top \zeta \\ \text{subject to:} & F_{\mathcal{Z}_B(\theta, \mathcal{D}_p, k, \gamma_k)}^{-1}(1 - \zeta_k) \leq 0, \quad k = 1, \dots, n_r, \end{aligned} \quad (14)$$

where $\rho \in \mathbb{R}^{n_r}$ is the penalty parameter, $\zeta \in \mathbb{R}^{n_r}$ is a slack variable,

$$\mathcal{Z}_B(\theta, \mathcal{D}_p, k, \gamma_k) \triangleq \left\{ F_{\mathcal{Z}_A(\theta, \delta_p^{(i)}, k)}^{-1}(\gamma_k) \right\}_{i=1}^n, \quad (15)$$

is the sequence of the γ_k -quantiles for the k th requirement for all perturbed scenarios, and \mathcal{Z}_A is in (10). Hence, (14) seeks a design that minimizes the sum of J and a penalty term while making the $1 - \zeta_k$ quantile of $\mathcal{Z}_B(\theta, \mathcal{D}_p, k, \gamma_k)$ for all $k = 1, \dots, n_r$ fall into the success domain. As before, this is a flexible scheme that enables the analyst to explore various solutions as $\|\rho\|$ is varied from zero to infinite. Large values of $\|\rho\|$ will make ζ_k^* approach zero, thereby ensuring that as many individual probabilities of success as possible are acceptably large. Smaller values of $\|\rho\|$ will yield designs for which only a fraction of such probabilities does so. The outliers of (14) are also defined by (11).

Note that ζ_k^* is the fraction of the scenarios for which the probability of success for the k th requirement is less than γ_k . Further notice that making all the components of ρ equal gives the same importance to all the requirements. The relaxation of the CC by means of the tunable ζ prevents (14) from becoming infeasible. Designs resulting from (9) are generally different from those based on (14) because they use different loss measures. In particular,

ξ_i^* takes on a value in the positive range of the requirement functions whereas ζ_k^* takes on a value in $[0, 1]$. More importantly, the number of decision variables and the number of constraints in (14) depend on the number of requirements n_r instead of the number of scenarios n in (9), thereby having a lower the computational cost, e.g., the number of finite differences per design evaluation required by (14) is $(n_r + 1) \times (n_\theta + n_r)$ whereas that for (9) is $(n n_r + 1) \times (n_\theta + n)$.

A key benefit of the free relaxation carried out by the risk-averse formulations is that they permit seeking designs that can only satisfy the requirements for a subset of the scenarios without having any prior information about this subset. However, their risk-averse nature often renders a greater objective value. Conversely, the formulations that follow do not use a loss measure to carry out the relaxation, thereby becoming practically risk-agnostic. These formulations enable the analyst to prescribe upfront the desired number of outliers, i.e., the number of elements of A in (12), as well as the fraction of the perturbations allowed to violate the requirements, i.e., the number of elements of B in (12). This property yields the name “fixed” used hereafter. Note however that setting an overly small number of outliers will make the optimization program infeasible^f.

More importantly, fixed relaxations often yield lower objective values than their free counterparts. This is the result of the scenarios chosen as outliers falling in the upper quantiles of the distribution of the requirement functions, thereby yielding the greatest expansion of the feasible space. These formulations also have the advantage of having a number of decision variables that does not increase with the number of scenarios or the number of requirements. This feature is critical to the non-convex CC programs commonly found in many engineering applications.

V.C. Risk-agnostic Scenario-based Formulation

The extension of (13) and (9), for which $\gamma_k = 1$ or $\gamma_k < 1$ for all $k = 1, \dots, n_r$ respectively, is

$$\begin{aligned} \theta^* &= \underset{\theta \in \Theta}{\operatorname{argmin}} && J(\theta) \\ &\text{subject to:} && F_{\mathcal{Z}_C(\theta, \mathcal{D}_p)}^{-1}(1 - \alpha) \leq 0, \end{aligned} \quad (16)$$

where

$$\mathcal{Z}_C(\theta, \mathcal{D}_p) \triangleq \left\{ \max_{k=1, \dots, n_r} F_{\mathcal{Z}_A(\theta, \delta_p^{(i)}, k)}^{-1}(\gamma_k) \right\}_{i=1}^n, \quad (17)$$

is the sequence of the greatest quantiles from all requirements for all scenarios, and $0 \leq \alpha \ll 1$ is the fraction of the n scenarios to be considered as outliers. Hence, θ^* minimizes J while ensuring that $[100(1 - \alpha)]\%$ of the perturbed scenarios satisfy the requirements with an admissibly large probability of success.

^fInfeasibility is avoided by first solving a risk-averse formulation with $\rho \gg 1$ and choosing $\alpha = n_o/n$. Alternatively, the analyst can make α an additional decision variable in (16) or (18), and use $J(\theta) = \|\alpha\|_2$ to first obtain α^* . Any future choice of α satisfying $\alpha \leq \alpha^*$ will make such a program feasible.

V.D. Risk-agnostic Requirement-based Formulation

The extension of (14) is

$$\begin{aligned} \theta^* &= \operatorname{argmin}_{\theta \in \Theta} J(\theta) \\ \text{subject to: } & F_{\mathcal{Z}_B(\theta, \mathcal{D}_p, k, \gamma_k)}^{-1}(1 - \alpha_k) \geq 0, \quad k = 1, \dots, n_r, \end{aligned} \quad (18)$$

where \mathcal{Z}_B is in (15), and $0 \leq \alpha_k \ll 1$ is the fraction of the n scenarios violating the CC for the k th requirement. Hence, θ^* minimizes J while ensuring that $\lceil 100(1 - \alpha_k) \rceil\%$ of the n probabilities of success for all $k = 1, \dots, n_r$ requirements are acceptably large. Note that the outliers violating a requirement might be different from the outliers violating another requirement, and $\lceil \max_k \alpha_k \rceil \leq n_o/n \leq \lceil \sum \alpha_k \rceil$.

Designs based on (16) and (18) are practically risk-agnostic because θ^* will not depend on more than a single outlier, i.e., the scenario at which \mathcal{Z}_C takes the positive value closest to zero. This is a consequence of the number of scenarios prescribing the value of the inverse CDF in (32), which is equal to one when α is a multiple of $1/(n - 1)$ or two otherwise.

Example 1 (Data Enclosure Design): Next we use a toy problem in $n_\delta = 2$ dimensions to illustrate key features of the above formulations. In particular, we seek a set of minimal volume that encloses a set of aleatory points in \mathcal{D} . The requirement functions defining this set are

$$r_1(\theta, \delta) = \|\delta - c_1\|_2 - u_1 \leq 0, \quad (19)$$

$$r_2(\theta, \delta) = u_2 - \|\delta - c_2\|_2 \leq 0, \quad (20)$$

$$r_3(\theta) = \|c_2 - c_1\|_2 - u_1 \leq 0, \quad (21)$$

where $c_1 \in \mathbb{R}^{n_\delta}$, $c_2 \in \mathbb{R}^{n_\delta}$, $u_1 \geq 0$ and $u_2 \geq 0$ are the decision variables, i.e., $\theta = [c_1, u_1, c_2, u_2]$. Hence, the success domain $\mathcal{S}(\theta)$ is comprised of the points inside the circle $C_1 = \{\delta : r_1(\theta, \delta) \leq 0\}$ and outside the circle $C_2 = \{\delta : r_2(\theta, \delta) \leq 0\}$ such that the center of C_2 is in C_1 . Our goal is to find the design point θ leading to a $\mathcal{S}(\theta)$ of minimal volume that encloses (most of) the scenarios in \mathcal{D} and their vicinity.

This volume is computed using

$$J(\theta) = \operatorname{Vol}(\Delta) F_{Z(\theta, \mathcal{U})}(0), \quad (22)$$

where $Z(\theta, \mathcal{U}) = \{\max_{k=1,2} r_k(\theta, u^{(i)})\}_{i=1}^{n_u}$, and the elements of $\mathcal{U} = \{u^{(i)}\}_{i=1}^{n_u}$ are samples uniformly distributed in Δ . To start, we assume that \mathcal{D} contains $n = 15$ nominal scenarios.

Table 1: Figures of merit for several designs. The area of the success domain is evaluated using $n_u = 2 \times 10^4$ sample points.

	θ_1^*	θ_2^*	θ_3^*	θ_4^*	θ_5^*	θ_6^*	θ_7^*	θ_8^*	θ_9^*	θ_{10}^*
Formulation	(13)	(13)	(16)	(16)	(13)	(13)	(9)	(9)	(18)	(18)
m	1	1	1	1	81	81	81	81	81	81
n_o	0	1	1	2	0	1	0	1	1	2
$J(\theta^*)$	11.26	10.53	8.30	7.79	15.13	14.97	14.63	13.41	9.64	6.57

Two multi-point designs, denoted as θ_1^* and θ_2^* , derived from the worst-case formulation (13) for $m = 1$ are presented first. The top subplots in Figure 1 show their corresponding

success and failure domains along with the nominal scenarios. Whereas $\mathcal{S}(\theta_1^*)$ encloses all the scenarios, $\mathcal{S}(\theta_2^*)$ excludes an outlier. Table 1 lists relevant metrics for these and other designs. Because the formulation is risk-averse, the elimination of the outlier rendered a small reduction in $J(\theta^*)$. This is the result of the penalty term in the objective function keeping the positive element of ξ^* near zero. Note that θ_1^* is not robust to perturbations in the data. For instance, most perturbations of the nominal scenario $\hat{\delta} = [-3.7, -0.4]$ fall onto the failure domain.

Two multi-point designs, denoted as θ_3^* and θ_4^* , derived from the risk-agnostic formulation (16) for $m = 1$ are presented next. The bottom subplots of Figure 1 show their corresponding success and failure domains. Whereas $\mathcal{S}(\theta_3^*)$ excludes a single outlier, $\mathcal{S}(\theta_4^*)$ excludes two outliers. Because this formulation is risk-agnostic, the elimination of the first outlier rendered a greater reduction in the objective value than θ_2^* . The elimination of the second outlier led to a slight improvement. However, all four designs are not robust to perturbations in the value of the nominal scenarios.

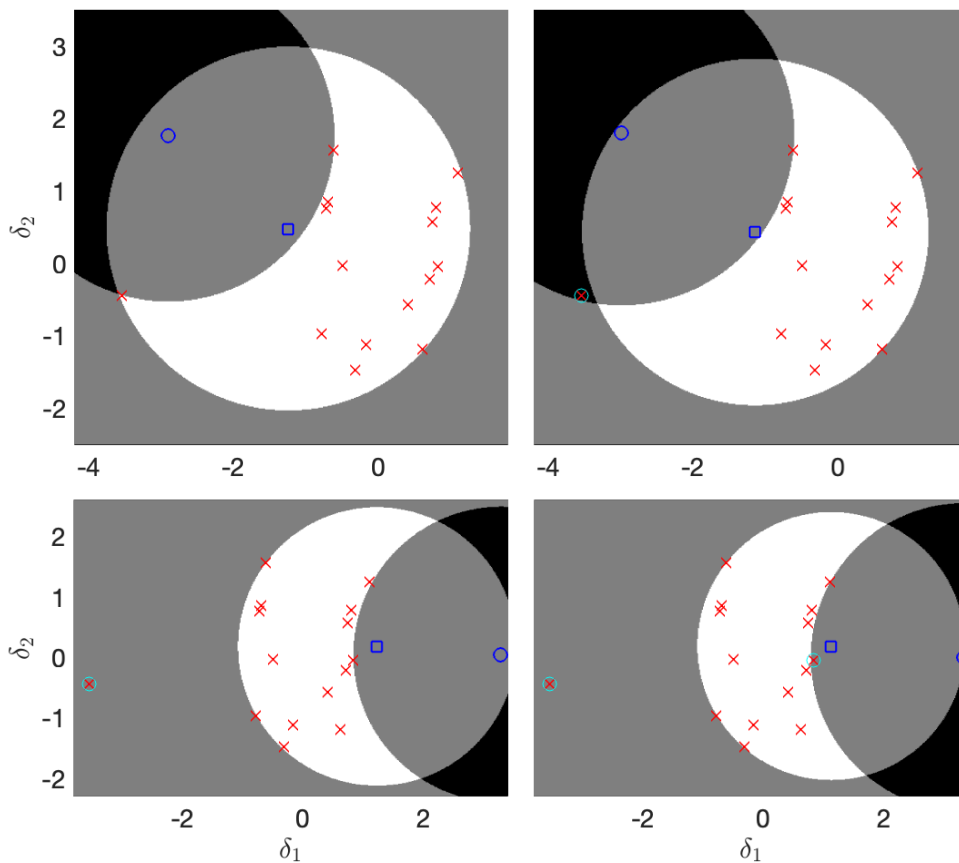


Figure 1: Success (white) and failure (non-white) domains for θ_1^* ($n_o = 0$), θ_2^* ($n_o = 1$), θ_3^* ($n_o = 1$) and θ_4^* ($n_o = 2$). The failure domain is shown in tones of gray: the darker the color the greater the number of constraint violations. The nominal scenarios are marked with a “x” whereas the scenarios falling into the failure domain are also marked with “o” (if any). The center c_1 is marked with a “□” whereas the center c_2 is marked with a “o”.

A few multi-point-robust designs are presented below. These designs are based on sequences having $m = 81$ points distributed over circular support sets having δ dependent radii.

These radii were chosen to depend on the distance from the nominal scenario to the origin. Two sample sets \mathcal{D}_p will be considered. The first sample set, shown in the top subplots of Figure 2, have points falling on the surface of the circles. This set is suitable for the worst-case formulation since the success domain is connected. The second sample set, shown in the middle and bottom subplots of Figure 2, have points falling on the area of the circles. This set is suitable for the CC formulation.

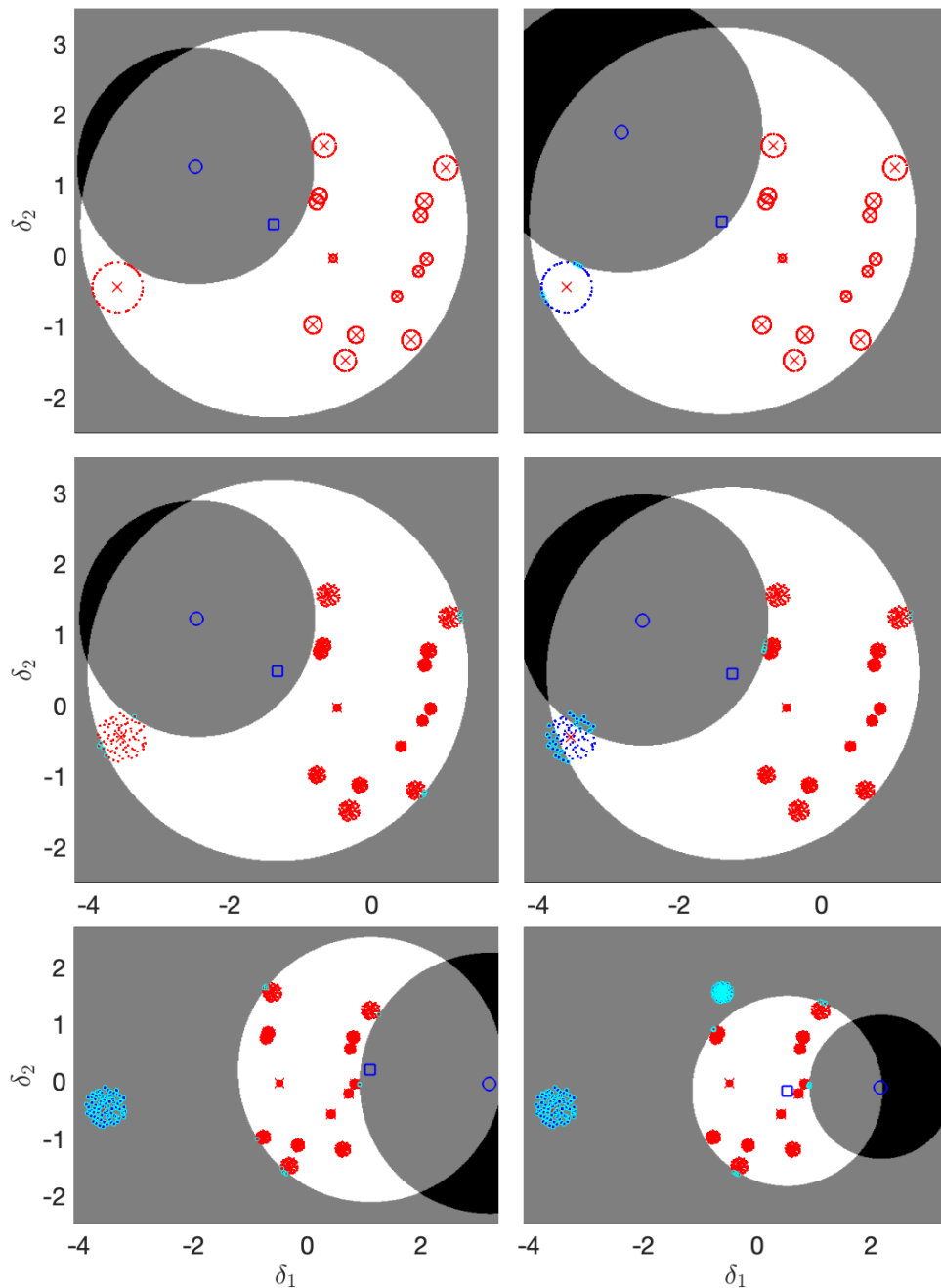


Figure 2: Success and failure domains for θ_5^* ($n_o = 0$), θ_6^* ($n_o = 1$), θ_7^* ($n_o = 0$), θ_8^* ($n_o = 1$), θ_9^* ($n_o = 1$) and θ_{10}^* ($n_o = 2$). The elements of $\delta_p^{(i)}$ corresponding to outliers are marked with a “x”, inliers are marked with a “o”, and elements falling into the failure domain are marked with a “•” (if any).

Two worst-case designs derived from (13), denoted as θ_5^* and θ_6^* hereafter, are presented first. The top subplots of Figure 2 shows that $\mathcal{S}(\theta_5^*)$ encloses all the perturbed scenarios, whereas $\mathcal{S}(\theta_6^*)$ excludes an outlier. As expected, the size of $\mathcal{S}(\theta_5^*)$ is greater than that of $\mathcal{S}(\theta_1^*)$, and the vicinity of $\hat{\delta}$ now falls into $\mathcal{S}(\theta_5^*)$. The relaxation caused by eliminating an outlier made a few points of such a scenario fall into $\mathcal{F}(\theta_6^*)$. However, the objective value only improved slightly. Designs θ_5^* and θ_6^* exhibit better robustness than their overfitting counterparts, but the loss measure in the penalty term prevents driving the scenario at $\hat{\delta}$ deeper into the failure domain, an outcome that would significantly lower $J(\theta^*)$.

Two designs based on the risk-averse formulation (9) with $\gamma_1 = \gamma_2 = 0.95$, denoted as θ_7^* and θ_8^* hereafter, are presented next. The parameter space corresponding to these designs are shown in the middle subplots of Figure 2. Whereas θ_7^* drives all perturbed scenarios into the success domain with a probability not less than 0.95, θ_8^* fails to do so for a single outlier. Note that a few points of three scenarios fall into $\mathcal{F}(\theta_7^*)$ even though $n_o = 0$. $J(\theta_8^*) < J(\theta_6^*)$ thanks to the expansion of the feasible set attained by the CCs, i.e., A in (12) was kept the same whereas B was reduced for a single scenario. By changing both ρ and γ the analyst can tune the robustness of a design.

Finally, the risk-agnostic formulation in (18) was used to derive θ_9^* and θ_{10}^* . The bottom subplots of Figure 2 show the corresponding parameter spaces. Whereas $\mathcal{S}(\theta_9^*)$ contains all but one perturbed scenarios with a probability no less than 0.95, $\mathcal{S}(\theta_{10}^*)$ excludes two scenarios. As before, a few points of 5 scenarios fall into $\mathcal{F}(\theta_9^*)$ even though $n_o = 0$. That is also the case for $\mathcal{F}(\theta_{10}^*)$, which contains points belonging to six perturbed scenarios. More importantly, note that both risk-agnostic optimal designs fully eliminate the effects of the outlier centered at $\hat{\delta}$, whose m points violate the first requirement by a large margin. This leads to reductions in the objective value of about 37.5% and 57.5% relative to θ_5^* . This illustrates how the elimination of the worst-performing scenarios enforced by the risk-agnostic formulations yields a considerably lower objective value than the risk-averse formulations. This feature, along with having a number of decision variables that does not scale with the number of scenarios, might make risk-agnostic approaches preferable. Recall, however, that such approaches often lead to non-convex optimization programs even when the requirements are convex.

VI. Moment-dependent Optimization Programs

In this section we consider problems that seek to minimize a moment of a response function. This is accomplished by using $J = \lambda$ and adding the constraint $\mathbb{M}[h(\theta, \delta)] < \lambda$ to (8), where \mathbb{M} is an empirical moment of a response function $h(\theta, \delta)$ and λ is a decision variable. A key objective of the forthcoming formulations is to optimally identify and eliminate the same set of outliers from all the constraints. Thus, outliers will either yield large requirement function values or strongly contribute to $\mathbb{M}[h(\theta, \delta)]$. To simplify the presentation we will focus on the empirical mean, but the extension to order moments can be easily made. Denote as $\mathbb{E}[h(\theta, \delta), \mathcal{D}_p, \mathcal{W}]$ an empirical moment of $h(\theta, \delta)$ based on the scenarios in \mathcal{D}_p and the weights in $\mathcal{W} = \{w^{(i)}\}_{i=1}^n$, i.e.,

$$\mathbb{E}[h(\theta, \delta), \mathcal{D}_p, \mathcal{W}] = \frac{1}{\sum w^{(i)} m} \sum_{i=1}^n \sum_{j=1}^m h(\theta, \delta^{(i,j)}) w^{(i)}. \quad (23)$$

VI.A. Risk-averse Formulation

Consider the optimization program

$$\begin{aligned} \langle \theta^*, \lambda^*, \xi^* \rangle = \operatorname{argmin}_{\theta \in \Theta, \lambda, \xi \geq 0} \quad & \lambda + \rho \sum_{i=1}^n \xi_i \\ \text{subject to:} \quad & \mathbb{E}[h(\theta, \delta), \mathcal{D}_p, \mathcal{W}] \leq \lambda, \\ & F_{\mathcal{Z}_A(\theta, \delta_p^{(i)}, k)}^{-1}(\gamma_k) \leq \xi_i, \quad i = 1, \dots, n, \quad k = 1, \dots, n_r, \end{aligned} \quad (24)$$

where $\mathcal{W} = \{\exp(-\kappa \xi_i)\}_{i=1}^{n_a}$ for $\kappa \geq 1$ and \mathcal{Z}_A is in (10). Note that \mathcal{W} evaluated at ξ^* assigns a weight of one to the inliers and a weight near zero to the outliers. By making the weights depend smoothly on the decision variable ξ , gradient based algorithms are applicable. Hence, (24) seeks a design θ^* that minimizes the empirical mean of the response for the inliers and a penalty term subject to the same CCs considered earlier. Note that the slack variable ξ enables eliminating the same set of outliers from the mean and the constraints. In spite of this benefit, however, the risk-averse designs resulting from (24) exhibit the subpar performance and high cost discussed above.

VI.B. Risk-agnostic Formulation

Note that the decision variable ξ used to consistently eliminate outliers in (24) is unavailable. A risk-agnostic formulation based on (16) is presented next. Consider the moment sequence

$$\mathcal{Z}_E(\theta, \mathcal{D}_p) \triangleq \left\{ \mathbb{E}[h(\theta, \delta), \mathcal{D}_p, \{K_{ik}\}_{k=1}^n] \right\}_{i=1}^n, \quad (25)$$

where $\mathbb{E}[\cdot]$ was defined in (23) and K is the Kronecker delta. Hence, the i th element of \mathcal{Z}_E is an empirical mean of the response for all m sample points of the perturbed scenario $\delta_p^{(i)}$. Furthermore, define $\mathcal{Z}(i)$ as the subsequence of \mathcal{Z}_E whose n_i values do not exceed the i th-order statistic of \mathcal{Z}_E , and $g \in \mathbb{R}^{n_r+1}$ as

$$g(i, \theta, \lambda, \mathcal{D}_p, \gamma) \triangleq \left[\overline{\mathcal{Z}}(i) - \lambda, \quad F_{\mathcal{Z}_A(\theta, \delta_p^{(i)}, k)}^{-1}(\gamma_k) \text{ for } k = 1, \dots, n_r \right], \quad (26)$$

for $i = 1, \dots, n$. Hence, a scenario i^* for which $g(i^*, \theta, \lambda, \mathcal{D}_p, \gamma) \leq 0$ satisfies two properties. First, the mean of the response for the lowest n_{i^*} elements of \mathcal{Z}_E does not exceed λ . Second, i^* is an inlier. This sets the stage for the optimization program

$$\begin{aligned} \langle \theta^*, \lambda^* \rangle = \operatorname{argmin}_{\theta \in \Theta, \lambda} \quad & \lambda \\ \text{subject to:} \quad & F_{\mathcal{Z}_F(\theta, \lambda, \mathcal{D}_p, \gamma)}^{-1}(1 - \alpha) \leq 0, \end{aligned} \quad (27)$$

where $0 \leq \alpha \ll 1$ is the fraction of the n scenarios considered as outliers, and

$$\mathcal{Z}_F(\theta, \lambda, \mathcal{D}_p, \gamma) \triangleq \left\{ \max_{j=1, \dots, n_r+1} g_j(i, \theta, \lambda, \mathcal{D}_p, \gamma) \right\}_{i=1}^n. \quad (28)$$

Hence, (27) yields a design θ^* that minimizes the lowest sample moment of the response for $[100(1 - \alpha)]\%$ of the scenarios while ensuring that they satisfy the requirements with an acceptably large probability of success. The max operator in (28) ensures that the same set of outliers are removed from all the constraints. As before, the risk-agnostic formulation (27) often leads to a lower objective values than the risk-averse formulation (24).

VII. Reliability Analyses

The formulations above are based on computationally tractable heuristics for $\mathbb{P}_{\delta^{(i)}}[\mathcal{S}_k(\theta)] \geq \gamma_k$ with $k = 1, \dots, n_r$, and the training set of perturbed scenarios \mathcal{D}_p . However, without further analyses we cannot know if θ^* satisfies such constraints when $n \rightarrow \infty$. The extent by which these heuristics address the original problem is often evaluated by using either Monte Carlo analysis or scenario theory. A Monte Carlo analysis estimates the probability of requirement violations for any θ regardless of the means by which such a design was obtained. On the other hand, scenario theory yields a rigorous, distribution-free upper bound to this probability for scenario-based optimal designs.

In the developments that follow we will carry out two reliability analyses. The first analysis, which neglects the uncertainty in the data, evaluates the probability of nominal scenarios falling into the failure domain, i.e., $\mathbb{P}_\delta[\delta \in \mathcal{F}(\theta)]$. The second analysis, which accounts for uncertainty in the data, evaluates the probability of perturbed scenarios falling into the failure domain beyond an acceptable limit[§], i.e., $\mathbb{P}_\delta[\mathbb{P}_{\delta^{(i)}}[\delta^{(i)} \in \mathcal{F}(\theta)] > 1 - \gamma]$. These analyses will be referred to as nominal and perturbational respectively.

These probabilities can be readily evaluated using Monte Carlo. In the nominal case the process entails generating a testing dataset with $n' \gg 1$ nominal scenarios, and finding the fraction of such points falling onto $\mathcal{F}(\theta)$. In the perturbational case, the distribution δ_d in (6) corresponding to each of the n' scenarios is first simulated to obtain $m' \gg 1$ sample points. The desired probability is the fraction of the n' scenarios for which more than $\lceil m'(1 - \gamma) \rceil$ points fall onto $\mathcal{F}(\theta)$. Nominal and perturbational risk analyses can also be carried out using scenario theory. The developments in [66] are applicable to multi-point designs for which $m = 1$, whereas those in [79] can be extended to proposed multi-point-robust designs. These extensions, however, are omitted here due to space limitations.

Example 2 (Reliability Analyses of the Data Enclosing Sets): The designs presented in Example 1 are based on a small dataset thereby possibly exhibiting a large failure probability. Four designs based on a dataset having $n = 500$ scenarios and $\gamma = 0.95$ are presented next. In particular, we consider a multi-point-design with $n_o = 25$ outliers and $m = 1$, a multi-point design without outliers and $m = 1$, a multi-point-robust design with $n_o = 25$ outliers, and a multi-point-robust design without outliers. The resulting designs, denoted as θ_A^* , θ_B^* , θ_C^* and θ_D^* respectively, are based on formulation (16). In contrast to the perturbations \mathcal{D}_p used previously, we will consider adversarial perturbations. In particular, the radius of the circular perturbation for the i th scenario is

$$r^{(i)} = r_{\max} \exp\left(-\max_{k=1,2} r_k(\theta, \delta^{(i)})^2\right). \quad (29)$$

Therefore, the closer the nominal scenario is to the boundary of the failure domain the stronger the perturbation. Adversarial actions are an additional source of non-convexity.

Figure 3 shows the parameter spaces corresponding to the resulting designs. Such designs attain various degrees of performance and robustness depending upon the choices of m , n_o , γ , and r_{\max} made upfront.

The nominal and perturbational reliability analyses of the four designs are presented in Table 2, where the objective value, the desired failure probabilities and the confidence

[§]This probability, called the perturbational failure probability hereafter, will be denoted as $\mathbb{P}_{\delta^{(\gamma)}}[\mathcal{F}(\theta)]$ to simplify the notation.

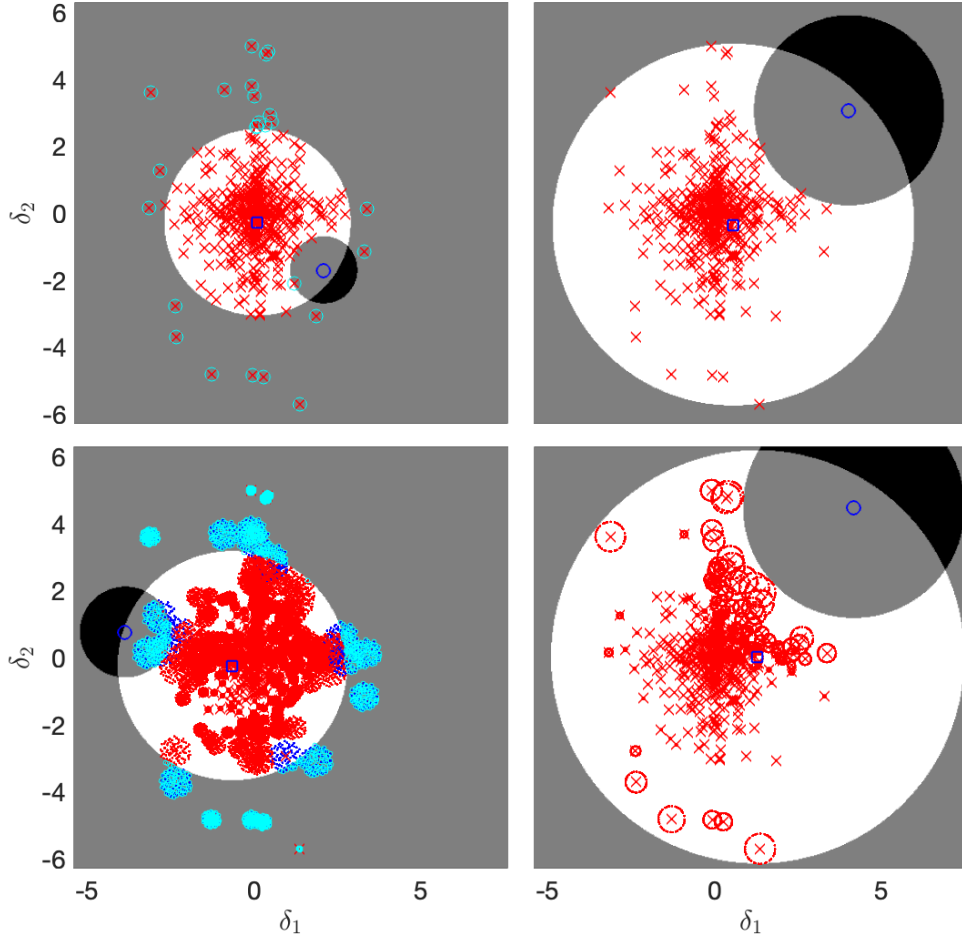


Figure 3: Success and failure domains for θ_A^* , θ_B^* , θ_C^* and θ_D^* .

Table 2: Performance and robustness metrics of several designs. $J(\theta^*)$ is the objective value, $\mathbb{P}_\delta[\mathcal{F}(\theta^*)]$ is the nominal failure probability, $\mathbb{P}_{\delta(\gamma)}[\mathcal{F}(\theta^*)]$ is the perturbational failure probability, and CI is the 95% confidence interval of this probability.

	m	n_o/n	$J(\theta^*)$	$\mathbb{P}_\delta[\mathcal{F}(\theta^*)]$	CI	$\mathbb{P}_{\delta(0.05)}[\mathcal{F}(\theta^*)]$	CI
θ_A^*	1	0.05	22.26	8.76×10^{-2}	$[8.35, 9.17] \times 10^{-2}$	1.46×10^{-1}	$[1.40, 1.50] \times 10^{-1}$
θ_B^*	1	0	77.68	1.60×10^{-2}	$[1.42, 1.78] \times 10^{-2}$	3.09×10^{-2}	$[2.87, 3.37] \times 10^{-2}$
θ_C^*	81	0.05	34.01	5.41×10^{-2}	$[5.09, 5.74] \times 10^{-2}$	8.34×10^{-2}	$[8.02, 8.83] \times 10^{-2}$
θ_D^*	81	0	91.36	8.95×10^{-3}	$[0.76, 1.03] \times 10^{-2}$	1.64×10^{-2}	$[1.47, 1.83] \times 10^{-2}$

intervals [81] are provided. These estimates are based on a Monte Carlo campaign with $n' = 20000$ nominal scenarios and $m' = 200$ sample points. As expected, the perturbational probabilities are greater than the nominal probabilities. The analyst should choose a design among the alternatives according to the desired balance between performance, as measured by a lower $J(\theta^*)$, and robustness, as measured by the failure probabilities. As expected, the performance-based ranking of the four designs is the opposite of the robustness-based ranking. Note that lowering the failure probability one order of magnitude increased the optimal objective value 4.13 times.

If the failure probability estimate found in testing is unacceptably large, a scenario program with a greater n could be computed. However, a small probability of failure requires a large training dataset, thereby increasing the computational cost of solving the corresponding scenario program. This cost becomes insurmountable in applications where the requirements must be evaluated by simulation. This outcome can be avoided by sequentially enlarging the dataset with a few scenarios falling into the failure domain of a baseline design (See next Section). This practice, however, violates the IID assumption on the data required by the scenario-based bound.

VIII. Robust Design of a Aeroelastic Wing

VIII.A. Problem Formulation

Next we consider the design of a flexible aeroelastic wing subject to static and dynamic structural requirements. The dimensions of the wing are set to emulate a subsonic wind tunnel test model [82]. The objective function to be minimized is the sample mean of a weighted combination of the structural wing mass, and the aerodynamic drag coefficient computed at a static aeroelastic trim condition, thereby making the developments of Section VI applicable. When a flexible wing is subjected to low dynamic pressures, structural dynamic perturbations will dampen out in time, thereby leading to an asymptotically stable response. At higher dynamic pressures, however, coupling between the structure and the unsteady aerodynamics might result in an unstable wing, where oscillations grow unbounded in time. This phenomenon is called aeroelastic flutter, and the first design requirement considered here, $r_1(\theta, \delta) < 0$, ensures that the wing does not flutter below some prescribed dynamic pressure threshold. The second design requirement, $r_2(\theta, \delta) < 0$, ensures that the static stresses which develop along the wing at the trim condition do not exceed a limit. Hence, the success domain, $\mathcal{S}(\theta)$, is comprised of the δ points for which the wing does not flutter, and the peak stress is acceptable. Our goal is to find the wing of minimal objective value that satisfies the requirements for most of the scenarios in \mathcal{D} and their vicinity.

The design variables $\theta \in \mathbb{R}^9$, shown in Figure 4, are segregated into shape and sizing variables. Four shaping variables prescribe the planform of the wing, by changing the root chord, the tip chord, the semispan, and the wing sweep. Each of these variables ranges from -5 to 5 inches, and additively scales the baseline wing shape. The baseline root chord is 22 inches, and so may vary during design from 17 to 27 inches. Similarly, the baseline tip chord is 14.5 inches, the baseline semispan is 30 inches, and the baseline wing sweep is 32 inches. In addition, we consider five structural sizing variables governing the plate thickness down the span of the wing, as shown in the figure. The spanwise thickness distribution is governed by a piecewise linear interpolation across the 5 control points. The baseline plate thickness is 1 inch, and may vary between 0.25 and 1.75 inches.

The aeroelastic constraints are detailed next. The function $r_1(\theta, \delta)$ is a dynamic aeroelastic constraint, and entails computing the flutter instability point, namely the flutter dynamic pressure, via a matched point $p-k$ scheme [83]. Hence, the constraint $r_1(\theta, \delta) \leq 0$ is satisfied when the flutter dynamic pressure exceeds a limiting value of 2 psi. The function $r_2(\theta, \delta)$ is a static aeroelastic constraint: using the wing angle of attack, the flexible wing is trimmed to a lift coefficient of 0.5 at a dynamic pressure of 1.5 psi. The elastic von-Mises stresses are then computed within the deformed wing, and these values are finally aggregated into

a single scalar output via the Kreisselmeier-Steinhauser method [84]. Hence, the constraint $r_2(\theta, \delta) < 0$ is satisfied when the stress aggregation function is less than the yield stress, i.e., all the finite elements are inside their failure envelope. The drag coefficient needed for the objective function is computed from the same trimmed state.

The parameter $\delta \in \mathbb{R}^6$ combines uncertain parameters and changing operating conditions. In particular, δ includes the Mach number of the static and dynamic aeroelastic physics, the mass-proportional Rayleigh damping coefficient, the stiffness-proportional Rayleigh damping coefficient, the kinematic viscosity of the flow, and the target lift coefficient for the trim state. These parameters vary uniformly over the hyper-rectangular set $[0.4, 0.9] \times [0, 25] \times [0, 0.001] \times [0.8 \times 10^{-5} \text{ to } 1.2 \times 10^{-5}] \times [0.4, 0.6]$ respectively. As such, the scenarios to be used for design and testing are obtained synthetically from an assumed distribution.

The underlying structural wing model is idealized as a flat plate shell cantilevered along its root, and immersed in subsonic flow. The structure of the wing is modeled with a linear shell finite element model, and both the steady and unsteady aerodynamics are modeled with the linear doublet lattice method [85]. A finite plate spline [86] is used to pass wing deformations from the structure to the aerodynamics, as well as loads from the aerodynamics to the structure. Given that only linear compressible aerodynamics are utilized here, this solver will become less accurate as the Mach number approaches unity, and aerodynamic nonlinearities become more prominent. Nonlinear flow solvers (i.e., computational fluid dynamics) could be used for higher accuracy, but at a much greater computational cost [87].

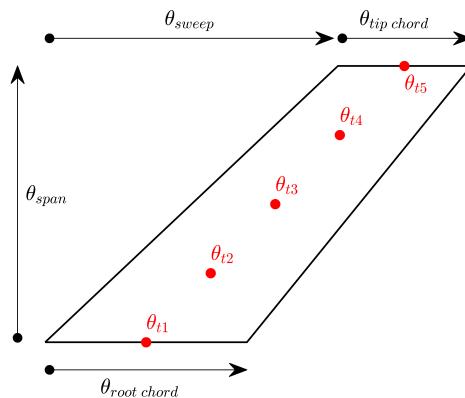


Figure 4: Shape and sizing design variables for the aeroelastic wing.

VIII.B. Wing Design Candidates

A single-point wing design is presented first. This design, obtained from (13) for $\mathcal{D} = \{\delta_{nom}\}$, will be denoted as θ_1^* . As expected, single-point designs might not satisfy the desired specifications. To improve the robustness of single-point designs, the analyst might consider using what he/she believes is the worst-case combination of uncertainties as δ_{nom} . This practice might render a conservative design having an overly large objective value. It is also possible for the resulting design to be insufficiently robust since such a combination usually depends non-trivially on θ and the requirement functions. As such, multi-point approaches are preferable.

Two multi-point designs based on a training dataset \mathcal{D} with $n = 50$ scenarios and $m = 1$ are presented next. A relatively small number of training scenarios is chosen due to the high computational cost of performing an aeroelastic analysis within the optimization loop. In particular, design θ_2^* was computed using (9) with $J = 0$, $\gamma_1 = \gamma_2 = 1$. Hence, this design maximizes the probability of success for the nominal scenarios. Design θ_3^* was computed using (27) for $\alpha = 0$. Hence, this design minimizes the sample mean of the response for the nominal scenarios while ensuring that they satisfy the requirements. Figure 5 shows these and other wing designs.

Prominent features of the resulting designs are discussed next. In an effort to minimize the structural mass, each design decreases the root and tip chord length, and also decreases the structural thickness at the tip. A tapered thickness profile from root to tip is driven by a reduction in static stresses down the span. Each optimal wing design is unswept relative to the baseline design, shown to the left of Figure 5, a change that helps to satisfy the flutter constraint without increasing the structural mass. The multi-point designs θ_2^* and θ_3^* exhibit a large increase in the structural root thickness, which in turn lower the failure probability relative to θ_1^* while increasing the objective value.

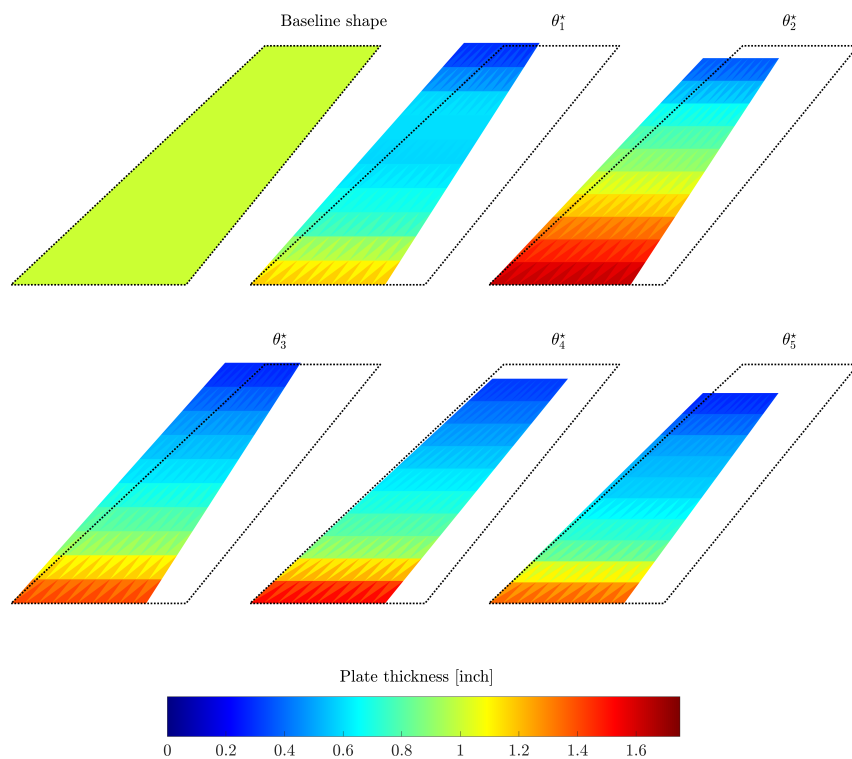


Figure 5: Optimal wing designs. The dashed black line indicates the baseline planform shape used for reference.

VIII.C. Reliability Analysis

A nominal reliability analysis of such wing designs is presented next. This analysis, whose results are shown in Table 3, is carried out by using a Monte Carlo campaign with $n' = 1 \times 10^4$ nominal scenarios. Note that the 2nd, 3rd and 4th columns correspond to the training dataset \mathcal{D} whereas the last six columns correspond to the testing dataset \mathcal{D}' . As expected, the large

failure probabilities of θ_1^* make it unsuitable. That is not the case for θ_2^* which meets the requirement for all scenarios in both the training and testing datasets. Note that a failure probability of zero based on $n' = 1 \times 10^4$ testing scenarios was attained by only using 50 training scenarios. This outcome, however, is fortuitous. Recall that θ_2^* does not seek to lower the objective function value but instead focuses on satisfying the requirements for all scenarios. This is not the case for θ_3^* , which lowers the objective function to 3.25 while satisfying the requirements for the training set. Note however that the reliability analysis reveals failure probabilities greater than zero. This discrepancy is caused by such a design overfitting the $n = 50$ training scenarios. As expected, lowering the objective value and satisfying the requirements robustly are conflicting objectives.

Table 3: Nominal reliability analysis and supporting information: n is the number of scenarios used for training, m is the number of perturbations per scenario, n_o is the number of outliers, $\mathbb{E}_\delta[f|I]$ is the empirical mean for the non-outlying scenarios in the training set, $\mathbb{E}_\delta[f]$ is the empirical mean, $P_\delta[\mathcal{F}_i]$ is the failure probability for the i th requirement, $P_\delta[\mathcal{F}]$ is the total failure probability, and $\ell_i = \mathbb{E}[r_i(\theta, \delta) | r_i(\theta, \delta) > 0]$ is a loss measure. The last six columns use a testing dataset \mathcal{D}' having $n' = 1 \times 10^4$ scenarios.

	n	m	n_o	$\mathbb{E}_\delta[f I]$	$\mathbb{E}_\delta[f]$	$P_\delta[\mathcal{F}_1]$	$P_\delta[\mathcal{F}_2]$	$P_\delta[\mathcal{F}]$	ℓ_1	ℓ_2
θ_1^*	1	1	0	3.08	3.12	3.75×10^{-1}	4.81×10^{-1}	6.73×10^{-1}	0.072	0.127
θ_2^*	50	1	0	3.80	3.81	0	0	0	0	0
θ_3^*	50	1	0	3.25	3.25	9.20×10^{-3}	6.90×10^{-3}	1.60×10^{-2}	0.011	0.012
θ_4^*	50	[1,2]	0	3.31	3.31	3.70×10^{-3}	1.00×10^{-4}	3.80×10^{-3}	0.088	0.001
θ_5^*	67	1	0	3.33	3.28	0	0	0	0	0

A multi-point-robust design, seeking to improve the robustness of θ_3^* , is developed next. Given the high computational cost of evaluating the requirement functions, we will only perturb some of the nominal scenarios. These perturbations are worst-case in the δ continuum. The worst-case perturbation of the nominal scenario $\hat{\delta}$ with respect to the requirement r_k for the design $\hat{\theta}$ is

$$\delta_w(\lambda, k, \hat{\delta}, \hat{\theta}) = \hat{\delta} + \lambda \left. \frac{\partial r_k(\theta, \delta)}{\partial \delta} \right|_{\hat{\delta}, \hat{\theta}}, \quad (30)$$

where $\lambda > 0$. Hence, δ_w is in the direction of the gradient of the k th requirement function evaluated at $\hat{\delta}$ and $\hat{\theta}$. The decision point $\hat{\theta}$ where the gradient is evaluated might be kept fixed, say at the value of θ corresponding to a baseline design; or it might be sequentially updated as the optimization algorithm converges to θ^* . The later option, which constitutes an adversarial perturbation, is computationally appealing because the satisfaction of the requirements at this perturbation implies that for other neighboring perturbations. This setting is particularly suitable when automatic differentiation is available. Furthermore, we will choose $\hat{k} = \operatorname{argmax}_k r_k(\hat{\theta}, \delta)$ in (30) to ensure that δ is perturbed in the direction of the gradient of the worst-case requirement.

In the developments that follow, the only scenarios perturbed are those for which $r_{\hat{k}}(\hat{\theta}, \delta^{(i)})$ takes on the greatest non-negative values, and this perturbation is $\delta_w(\delta^{(i)}, \lambda, \hat{k}, \hat{\theta})$. Hence, the perturbed scenarios are the closest to the failure domain $\mathcal{F}_{\hat{k}}(\hat{\theta})$. The resulting sample sequence of worst-case perturbations will be denoted by $\mathcal{D}_p(\mathcal{M}, \hat{k}, \hat{\theta})$, where the i th element of $\mathcal{M} = \{m^{(i)}\}_{i=1}^{50}$ is the number of times the i th scenario is perturbed.

Formulation (27) with $\alpha = 0$ was used to synthesize the multi-point-robust wing θ_4^* using

the training dataset $\mathcal{D}_p(\mathcal{M}, \hat{k}, \theta_3^*)$. Whereas 46 elements of \mathcal{M} take the value of one, four elements take the value of two (recall that $\delta^{(i)} \in \mathcal{D}_p$ so $m = 1$ correspond to unperturbed parameters). Therefore, only four scenarios are perturbed from their nominal value. These four scenarios attain the greatest $r_{\hat{k}}(\theta_3^*, \delta^{(i)})$ negative values. Therefore, θ_4^* seeks to improve the robustness of θ_3^* without significantly increasing the computational cost required for its calculation. Figures of merit corresponding to the wing design θ_4^* , also shown in Figure 5, are also listed in Table 3. This wing not only meets the training specifications but also exhibits better robustness properties than θ_3^* . In particular, θ_4^* reduces the failure probability by a factor of 4.88 in exchange for a objective value increase of less than 2%. This is achieved without significantly increasing the strength of the flutter instability. Note that 4 additional training scenarios were needed to attain a 13% reduction in the objective value for a failure probability of 3.80×10^{-3} .

This example uses perturbational data as an artifact for increasing the robustness of a baseline design. As such, a prescription of \mathcal{D}_d and the corresponding perturbational reliability analysis are omitted.

VIII.D. Sequential Data-driven Design

In designing a more robust wing one could append to the starting training dataset some of testing scenarios falling into the failure region of a baseline design, thereby leveraging the results and computational effort of the reliability analysis. To this end, we use formulation (16) with $m = 1$, $\gamma_1 = \gamma_2 = 1$ for a dataset with $n = 67$ scenarios. The 17 scenarios added to the original sequence of 50 scenarios fall onto $\mathcal{F}(\theta_4^*)$ while attaining small $\min_k r_k(\theta_4^*, \delta^{(i)})$ values. The resulting design, denoted as θ_5^* , drives the failure probability to zero while attaining a much smaller objective value than θ_2^* (See Table 3). Figure 5 shows that the most robust designs, θ_2^* and θ_5^* , differ significantly.

Figure 6 shows the probability of failure against the normalized expected response for the 5 wing designs. This figure not only shows the empirical estimates corresponding to the testing dataset but also the corresponding 95% confidence intervals. The volume of these intervals, which lead to the rectangles shown, approaches zero as the number of samples approaches infinity. Note that both θ_2^* and θ_5^* drive the failure probability to zero but the latter does it by only increasing the objective value 6%. This illustrates the potential drawbacks of designs focusing on satisfying the requirements only. Monte Carlo campaigns with a greater number of samples are required to reduce the width of the confidence intervals, thereby further discriminating θ_2^* from θ_5^* . The high computational cost of a simulation, however, might render this practice infeasible.

IX. Concluding Remarks

This paper proposes a scenario optimization framework to robust design in the presence of error and uncertainty in the data. The system's performance, as measured by the value taken by the objective function, and the system's robustness, as measured by the ability to satisfy the requirements for perturbations in the data, are traded off by using two types of relaxations. Specifically, the feasible set is expanded by not only eliminating outliers from the dataset but also replacing constraints for the worst-case perturbation with chance constraints. Furthermore, we study the effects that loss measures commonly used to select

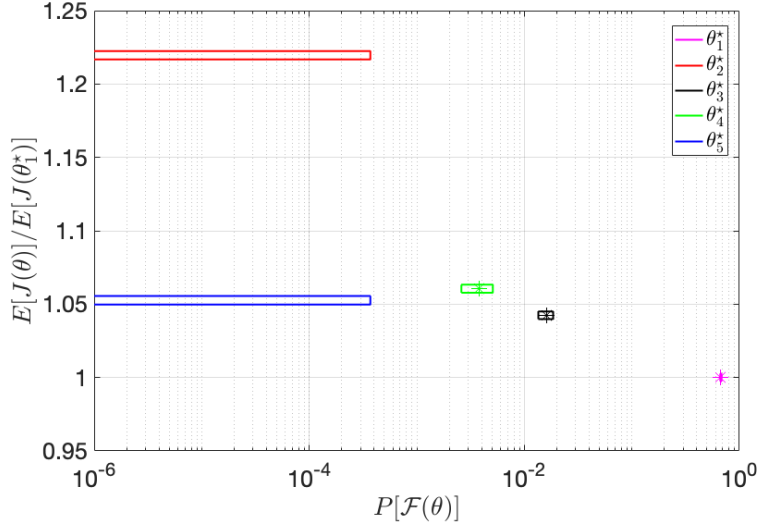


Figure 6: 95 confidence intervals of the probability of failure and the expected response based on a testing dataset with $n' = 1 \times 10^4$ samples. The empirical estimates corresponding to non-zero failure probabilities are shown as asterisks.

outliers have on the resulting design, and propose formulations that do not depend on any of them. The optimization programs proposed, some of which have a number of decision variables that do not increase with the number of scenarios, can be solved using standard gradient-based algorithms while being applicable to continuous but otherwise arbitrary requirement functions. This setting is amenable to many problems in science and engineering for which the objective function and constraints must be evaluated by simulation. Furthermore, these strategies can be naturally integrated to the Monte Carlo campaigns commonly used to evaluate a system's robustness by bridging the verification phase with the design phase.

In future work we will study the feasibility guarantees of scenario programs having CCs. Furthermore, we will develop strategies to systematically expand the training set in order to meet the reliability specifications imposed upon the system.

Appendix (CDF approximations)

Approximations to the CDF of a random variable and its inverse are presented next. Consider the non-decreasing sequence $\mathcal{Z} = \{z_i\}_{i=1}^n$ that results from evaluating the function $z(\theta, \delta)$ at $\{\delta^{(i)}\}_{i=1}^n$ for a fixed θ and sorting the resulting values so $z_i = z(\delta^{(j)})$ for some j and $z_i < z_{i+1}$. A continuous, piecewise linear approximation to the CDF of $z(\delta)$ based on $\mathcal{Z} = \{z(\delta^{(i)})\}_{i=1}^n$ is

$$F_{\mathcal{Z}(\theta)}(z) \triangleq \begin{cases} 0 & \text{if } z \leq z_1, \\ \frac{1}{n-1} \left(i - 1 + \frac{z - z_i}{z_{i+1} - z_i} \right) & \text{if } z_i < z \leq z_{i+1}, \\ 1 & \text{otherwise.} \end{cases} \quad (31)$$

The inverse of (31) is

$$F_{\mathcal{Z}(\theta)}^{-1}(\alpha) = \begin{cases} z_1 & \text{if } \alpha = 0, \\ z_i + (z_{i+1} - z_i) ((n-1)\alpha - i + 1) & \text{if } 0 < \alpha < 1, \\ z_n & \text{otherwise,} \end{cases} \quad (32)$$

where $\alpha \in [0, 1]$ and $i = \operatorname{argmin}_{j=1, \dots, n} \{(n-1)\alpha - j + 1 : j - 1 \leq \alpha(n-1)\}$. The approximations (31) and (32) are differentiable in θ when $z(\theta, \delta)$ is C^1 in θ . This property makes standard gradient-based algorithms applicable to the above optimization programs. When \mathcal{Z} contains repeated values, (31) and (32) can be used after breaking the ties with small perturbations.

Acknowledgements

This work was supported by the NASA Human Research Program (HRP) for radiation protection.

References

- ¹ G. Dantzig, Linear programming under uncertainty, *Management Science* 1 (3) (1955) 197–206.
- ² A. Charnes, W. Cooper, Chance-constrained programming, *Management Science* 6 (1) (1959) 73–79.
- ³ A. Soyster, Convex programming with set-inclusive constraints and applications to inexact linear programming, *Operations Research* 1 (3) (1955) 1154–1157.
- ⁴ J. Mayer, P. Kall, *Stochastic linear programming: Models, theory and Computation*, Springer Verlag, 2010.
- ⁵ D. Bertsimas, A. Thiele, *Robust and data-driven optimization: Modern decision making under uncertainty*, INFORMS (2014).
- ⁶ L. El-Ghaoui, F. Oustry, H. Lebret, Robust solutions to uncertain semidefinite programs, *SIAM journal of optimization* 9 (1998) 33–52.
- ⁷ A. Ben-Tal, A. Nemirovski, Robust solutions of linear programming problems contaminated with uncertain data, *Mathematical Programming* 88 (2000) 411–424.
- ⁸ D. Bertsimas, D. Pachamanova, M. Sim, Robust linear optimization under general norms, *Operation Research Letters* 32 (6) (2004) 510–516.
- ⁹ A. Ben-Tal, L. E. Ghaoui, A. Nemirovski, *Robust Optimization*, Princeton University Press, 2009.
- ¹⁰ D. Bertsimas, D. Brown, C. Caramanis, *Theory and applications of robust optimization*, SIAM review (2011).

- ¹¹ A. Shapiro, D. Dentcheva, A. Ruszczyński., Lectures on stochastic programming: modeling and theory, SIAM, Philadelphia, PA, 2009.
- ¹² D. Coit, E. Zio, The evolution of system reliability optimization, *Reliability Engineering and System Safety* 192 (2019) 106259.
- ¹³ M. Tsatsanis, Z. Xu, Performance analysis of minimum variance cdma receivers, *IEEE Transactions on Signal Processing* 46 (11) (1998) 3014–3022. doi:10.1109/78.726814.
- ¹⁴ M. K. Mehlawat, P. Gupta, A. Z. Khan, Portfolio optimization using higher moments in an uncertain random environment, *Information Sciences* 567 (2021) 348–374.
- ¹⁵ J. Hammond, L. Crespo, F. Montemoli, A distributionally robust data-driven framework to reliability analysis, *Structural Safety* 111 (102501) (2024).
- ¹⁶ J. Luedtke, S. Ahmed, G. Nemhauser, An integer programming approach for linear programs with probabilistic constraints, in: *Mathematical Programming*, Vol. 122, 2010, pp. 247–272.
- ¹⁷ F. Qiu, S. Ahmed, S. S. Dey, L. A. Wolsey, Covering linear programming with violations, *INFORMS Journal on Computing* 26 (3) (2014) 531–546.
- ¹⁸ M. Chapman, M. Faub, K. Smith, On optimizing the conditional value-at-risk of a maximum cost for risk-averse safety analysis, *IEEE Transactions on Automatic Control* (2022).
- ¹⁹ C. M. Lagoa, On the convexity of probabilistically constrained linear programs, in: *Proceedings of the 38th IEEE Conference on Decision and Control* (Cat. No.99CH36304), Vol. 1, 1999, pp. 516–52.
- ²⁰ G. Calafiore, M. Campi, The scenario approach to robust control design, *IEEE Transactions on automatic control* 51 (1) (2006) 742–753.
- ²¹ R. Henrion, C. Strugarek, Convexity of chance constraints with independent random variables, *Computational Optimization and Applications* 41 (2008) 263–276.
- ²² R. Henrion, C. Strugarek, *Convexity of Chance Constraints with Dependent Random Variables: The Use of Copulae*, Springer New York, New York, NY, 2011, pp. 427–439.
- ²³ A. Prekopa, K. Yoda, M. M. Subasi, Uniform quasi-concavity in probabilistic constrained stochastic programming, *Operations Research Letters* 39 (3) (2011) 188–192.
- ²⁴ W. van Ackooij, Eventual convexity of chance constrained feasible sets, *Optimization* 64 (5) (2015) 1263–1284.
- ²⁵ X. Geng, L. Xie, Data-driven decision making in power systems with probabilistic guarantees: Theory and applications of chance-constrained optimization, *Annual Reviews in Control* 47 (2019) 341–363.
- ²⁶ M. Mammarella, V. Mirasierra, M. Lorenzen, T. Alamo, F. Dabbene, Chance-constrained sets approximation: A probabilistic scaling approach, *Automatica* 137 (2022) 110108.

- ²⁷ D. W. Coit, E. Zio, The evolution of system reliability optimization, *Reliability Engineering & System Safety* 192 (2019) 106259.
- ²⁸ I. Enevoldsen, J. Sørensen, Reliability-based optimization in structural engineering, *Structural Safety* 15 (3) (1994) 169 – 196.
- ²⁹ X. Yuan, Z. Lu, Efficient approach for reliability-based optimization based on weighted importance sampling approach, *Reliability Engineering & System Safety* 132 (2014) 107 – 114.
- ³⁰ S. Shan, G. G. Wang, Reliable design space and complete single-loop reliability-based design optimization, *Reliability Engineering & System Safety* 93 (8) (2008) 1218 – 1230.
- ³¹ Z. Meng, B. Keshtegar, Adaptive conjugate single-loop method for efficient reliability-based design and topology optimization, *Computer Methods in Applied Mechanics and Engineering* 344 (2019) 95 – 119.
- ³² Y. Wang, P. Hao, H. Yang, B. Wang, Q. Gao, A confidence-based reliability optimization with single loop strategy and second-order reliability method, *Computer Methods in Applied Mechanics and Engineering* 372 (2020) 113436.
- ³³ W. Yao, X. Chen, Y. Huang, M. van Tooren, An enhanced unified uncertainty analysis approach based on first order reliability method with single-level optimization, *Reliability Engineering & System Safety* 116 (2013) 28 – 37.
- ³⁴ A. Torii, R. Lopez, L. Miguel, A second order SAP algorithm for risk and reliability based design optimization, *Reliability Engineering & System Safety* 190 (2019) 106499.
- ³⁵ H.-S. Li, S.-K. Au, Design optimization using subset simulation algorithm, *Structural Safety* 32 (6) (2010) 384 – 392, modeling and Analysis of Rare and Imprecise Information.
- ³⁶ M. de Angelis, E. Patelli, M. Beer, Advanced line sampling for efficient robust reliability analysis, *Structural Safety* 52 (2015) 170 – 182.
- ³⁷ A. Chaudhuri, B. Kramer, K. E. Willcox, Information reuse for importance sampling in reliability-based design optimization, *Reliability Engineering & System Safety* 201 (2020) 106853.
- ³⁸ E. Nikolaidis, R. Burdisso, Reliability based optimization: A safety index approach, *Computers & Structures* 28 (6) (1988) 781 – 788.
- ³⁹ L. Cizelj, B. Mavko, H. Riesch-Oppermann, Application of first and second order reliability methods in the safety assessment of cracked steam generator tubing, *Nuclear Engineering and Design* (1994) 359–368.
- ⁴⁰ G. Schuëller, H. Pradlwarter, P. Koutsourelakis, A critical appraisal of reliability estimation procedures for high dimensions, *Probabilistic Engineering Mechanics* 19 (4) (2004) 463 – 474.
- ⁴¹ J. Li, D. Xiu, Evaluation of failure probability via surrogate models, *Journal of Computational Physics* 229 (23) (2010) 8966 – 8980.

- ⁴² P. Chen, A. Quarteroni, Accurate and efficient evaluation of failure probability for partial differential equations with random input data, *Computer Methods in Applied Mechanics and Engineering* 267 (2013) 233 – 260.
- ⁴³ B. Peherstorfer, B. Kramer, K. Willcox, Combining multiple surrogate models to accelerate failure probability estimation with expensive high-fidelity models, *Journal of Computational Physics* 341 (2017) 61 – 75.
- ⁴⁴ B. Peherstorfer, B. Kramer, K. Willcox, Multifidelity preconditioning of the cross-entropy method for rare event simulation and failure probability estimation, *SIAM/ASA Journal on Uncertainty Quantification* 6 (2) (2018) 737–761.
- ⁴⁵ N. Dige, U. Diwekar, Efficient sampling algorithm for large-scale optimization under uncertainty problems, *Computers & Chemical Engineering* 115 (2018) 431 – 454.
- ⁴⁶ M. Li, Z. Wang, Surrogate model uncertainty quantification for reliability-based design optimization, *Reliability Engineering & System Safety* 192 (2019) 106432.
- ⁴⁷ E. Ullmann, I. Papaioannou, Multilevel estimation of rare events, *SIAM/ASA J. Uncertain. Quantification* 3 (2015) 922–953.
- ⁴⁸ R. Rockafellar, J. Royset, On buffered failure probability in design and optimization of structures, *Reliability Engineering & System Safety* 95 (5) (2010) 499 – 510.
- ⁴⁹ S. Sarykalin, G. Serraino, S. Uryasev, Value-at-Risk vs. Conditional Value-at-Risk in Risk Management and Optimization, no. 2014, Institute for Operations Research and the Management Sciences (INFORMS), 2014, Ch. Chapter 13, pp. 270–294.
- ⁵⁰ Y. Ben-Haim, A non-probabilistic concept of reliability, *Structural Safety* 14 (4) (1994) 227 – 245.
- ⁵¹ Z. Meng, Z. Zhang, H. Zhou, A novel experimental data-driven exponential convex model for reliability assessment with uncertain-but-bounded parameters, *Applied Mathematical Modelling* 77 (2020) 773 – 787.
- ⁵² L. G. Crespo, B. K. Colbert, S. P. Kenny, D. P. Giesy, On the quantification of aleatory and epistemic uncertainty using sliced-normal distributions, *Systems & Control Letters* 134 (2019) 104560.
- ⁵³ R. Rocchetta, M. Broggi, E. Patelli, Do we have enough data? robust reliability via uncertainty quantification, *Applied Mathematical Modelling* 54 (2018) 710 – 721.
- ⁵⁴ G. Shafer, A mathematical theory of evidence turns 40, *International Journal of Approximate Reasoning* 79 (2016) 7 – 25.
- ⁵⁵ S. Ferson, V. Kreinovich, L. Ginzburg, D. S. Myers, K. Sentz, Constructing probability boxes and Dempster-Shafer structures, Vol. 835, Sandia National Laboratories, 2002.
- ⁵⁶ D. Dubois, H. Prade, Possibility theory, probability theory and multiple-valued logics: A clarification, *Annals of Mathematics and Artificial Intelligence* 32 (2001) 35–66.

- ⁵⁷ P. Walley, *Statistical Reasoning with Imprecise Probabilities*, Chapman & Hall/CRC Monographs on Statistics & Applied Probability, Taylor & Francis, 1991.
- ⁵⁸ L. Zadeh, Fuzzy sets, *Information and Control* 8 (3) (1965) 338 – 353.
- ⁵⁹ Z. Liu, Y. Liu, J. Dezert, F. Cuzzolin, Evidence combination based on credal belief redistribution for pattern classification, *IEEE Transactions on Fuzzy Systems* 28 (4) (2020) 618–631.
- ⁶⁰ M. Eldred, L. Swiler, G. Tang, Mixed aleatory-epistemic uncertainty quantification with stochastic expansions and optimization-based interval estimation, *Reliability Engineering & System Safety* 96 (9) (2011) 1092 – 1113, quantification of Margins and Uncertainties.
- ⁶¹ W. Xie, On distributionally robust chance constrained programs with Wasserstein distance, *Mathematical Programming* 186 (2021).
- ⁶² S. Nannapaneni, S. Mahadevan, Reliability analysis under epistemic uncertainty, *Reliability Engineering & System Safety* 155 (2016) 9 – 20.
- ⁶³ M. Campi, A. Care, S. Garatti, The scenario approach: A tool at the service of data-driven decision making, *Annual Reviews in Control* 52 (2021) 1–17.
- ⁶⁴ J. A. Paulson, A. Mesbah, Data-driven scenario optimization for automated controller tuning with probabilistic performance guarantees, *IEEE Control Systems Letters* 5 (4) (2021) 1477–1482.
- ⁶⁵ M. Campi, S. Garatti, A theory of the risk for optimization with relaxation and its application to support vector machines, *Journal of Machine Learning* 22 (288) (2021).
- ⁶⁶ S. Garatti, M. Campi, Risk and complexity in scenario optimization, *Mathematical Programming* 191 (1) (2022) 243–279.
- ⁶⁷ J. Luedtke, S. Ahmed, A sample approximation approach for optimization with probabilistic constraints, *SIAM Journal on Optimization* 19 (2) (2008) 674–699.
- ⁶⁸ A. Nemirovski, A. Shapiro, Convex approximations of chance constrained programs, *SIAM Journal on Optimization* 17 (4) (2007) 969–996.
- ⁶⁹ Z. Khorashadi, J. Nossent, B. Taddesse, B. W., V. G. A., Impact of measurement error and limited data frequency on parameter estimation and uncertainty quantification, *Environmental Modeling & Software* 118 (1) (2019) 188–194.
- ⁷⁰ V. Eck, J. Sturdy, Effects of arterial wall models and measurement uncertainties on cardiovascular model predictions, *Journal of Biomechanics* 50 (1) (2017) 188–194.
- ⁷¹ H. Cartens, X. Xia, S. Yadavalli, Measurement uncertainty in energy monitoring: Present state of the art, *Renewable and Sustainable Energy Reviews* 82 (3) (2018) 2791–2805.
- ⁷² L. G. Crespo, T. C. Slaba, S. P. Kenny, M. W. Swinney, D. P. Giesy, Calibration of a radiation quality model for sparse and uncertain data, *Applied Mathematical Modeling* 95 (2021) 734–759.

- ⁷³ H. Wang, O. Gramstad, S. Schär, S. Marelli, E. Vanem, Comparison of probabilistic structural reliability methods for ultimate limit state assessment of wind turbines, *Structural Safety* 111 (2024) 102502.
- ⁷⁴ X. Dong, Q. Jiang, J. Lian, Z. Miao, T. Yu, H. Zhou, Optimized identification process of equivalent wind load calculations for offshore wind turbines under standstill conditions, *Ocean Engineering* 312 (2024) 119043.
- ⁷⁵ A. Haftbaradaran, K. Martin, A background sample-time error calibration technique using random data for wide-band high-resolution time-interleaved adcs, *IEEE Transactions on Circuits and Systems II: Express Briefs* 55 (3) (2008) 188–194.
- ⁷⁶ A. Archimbaud, K. Nordhausen, A. Ruiz-Gazen, ICS for multivariate outlier detection with application to quality control, *Computational Statistics and Data Analysis* 128 (2018) 184–199.
- ⁷⁷ Y. Liang, A. Thavaneswaran, Z. Zhu, R. K. Thulasiram, M. E. Hoque, Data-driven adaptive regularized risk forecasting, in: *2020 IEEE 44th Annual Computers, Software, and Applications Conference*, 2020, pp. 1296–1301.
- ⁷⁸ L. Guan, R. Tibshirani, Prediction and outlier detection in classification problems, *Journal of the Royal Statistical Society, Series B* 84 (2) (2022).
- ⁷⁹ M. C. Campi, A. Care, L. G. Crespo, G. S. F. Ramponi, Risk analysis and robust design of data-driven models against adversarial actions, *Journal of Machine Learning Research* submitted (2025).
- ⁸⁰ L. G. Crespo, T. Slagel, S. Kenny, A scenario-based approach to robust control design, in: *CEAS EuroGNC*, 2024.
- ⁸¹ J. Hanson, B. Beard, Applying monte carlo simulation to launch vehicle design and requirement analysis, *NASA/TP* 2010 216447 (2010).
- ⁸² C. Yates, Agard standard aeroelastic configurations for dynamic response. candidate configuration i - wing 445.6, *NASA Technical Memorandum* 100492 1 (1) (1987).
- ⁸³ L. van Zyl, M. Maserumule, Divergence and the p-k flutter equation, *Journal of Aircraft* 38 (3) (2001).
- ⁸⁴ G. Kreisselmeier, R. Steinhauser, Systematic control design by optimizing a vector performance index, *International Federation of Active Controls Symposium on Computer-Aided Design of Control Systems* (1979).
- ⁸⁵ M. Blair, A compilation of the mathematics leading to the doublet lattice method, *WL-TR-92-3028* (1992).
- ⁸⁶ K. Appa, Finite-surface spline, *Journal of Aircraft* 26 (5) (1989).
- ⁸⁷ B. Stanford, A. Thelen, K. Jacobson, Multifidelity optimization with transonic flutter constraints, *AIAA Aviation Forum (AIAA paper 2024-4025)* (2024).